USGS-OFR-84-552

USGS-OFR-84-552

UNITED STATES
DEPARTMENT OF THE INTERIOR
GEOLOGICAL SURVEY

Rock property measurements on large-volume core samples from Yucca Mountain USW GU-3/G-3 and USW G-4 boreholes, Nevada Test Site, Nevada

by

Lennart A. Anderson

Open-File Report 84-552

This report is preliminary and has not been reviewed for conformity with U.S. Geological Survey editorial standards. Any use of trade names is for descriptive purposes only and does not imply endorsement by the U.S.G.S.

Prepared by the U.S. Geological Survey

for

Nevada Operations Office
U.S. Department of Energy
(Interagency Agreement DE-AI08-78ET44802)

Denver, Colorado

1984

HYDROLOGY DOCUMENT NUMBER 56

UNITED STATES
DEPARTMENT OF THE INTERIOR
GEOLOGICAL SURVEY

Rock property measurements on large-volume core samples from Yucca Mountain USW GU-3/G-3 and USW G-4 boreholes, Nevada Test Site, Nevada

by

Lennart A. Anderson

Open-File Report 84-552

CONTENTS

Page

Introduction---------- 1

Laboratory procedures for sample measurements---------- 3

Results of laboratory analyses of borehole USW GU-3/G-3 core samples-- 4

Density and porosity measurements---------- 5

Compressional sonic velocity---------- 11

Electrical measurements---------- 12

Results of laboratory analysis of borehole USW G-4 core samples------ 21

Density and porosity measurements---------- 21

Compressional sonic velocity---------- 27

Electrical measurements---------- 27

Discussion---------- 33

References---------- 39

ILLUSTRATIONS

Figure 1.--Map of the Nevada Test Site showing the locations of the Yucca Mountain USW GU-3/G-3 and USW G-4 boreholes---------- 2

Figure 2.--Density values for USW GU-3/G-3 core samples plotted as a function of depth of origin---------- 9

Figure 3.--Porosity and compressional sonic velocity values for USW GU3/G3 core samples plotted as a function of depth of origin---------- 10

Figure 4.--Resistivity values for USW GU-3/G-3 natural state and resaturated core samples plotted against depth of origin-- 16

Figure 5.--Induced polarization and specific capacity values for USW GU-3/G-3 core samples plotted against depth of origin----- 19

Figure 6.--Density values for USW G-4 core samples plotted against depth of origin---------- 24

Figure 7.--Porosity and compressional sonic velocity values for USW G-4 core samples plotted as a function of depth of origin--26

Figure 8.--Resistivity values for USW G-4 natural state and resaturated core samples plotted against depth of origin---------- 28

ILLUSTRATIONS--Continued

Page

Figure 9.--Induced polarization and specific capacity values for USW G-4 core samples plotted against depth of origin---------- 32

Figure 10.-Correlation between saturated bulk density (SBD) and porosity for the USW GU-3/G-3 and USW G-4 sample data sets based on a least squares fit---------- 34

Figure 11.-Correlation between velocity and porosity for the USW GU-3/G-3 and USW G-4 sample data sets based on a least squares fit---------- 36

Figure 12.-Correlation between resistivity and porosity for the USW GU-3/G-3 and USW G-4 sample data sets based on a least squares fit---------- 37

TABLES

Page

Table 1.--Values of natural bulk density, saturated bulk density, dry bulk density, grain density, water-accessible porosity, and compressional sonic velocity for samples from USW GU-3/G-3 borehole---------- 6

Table 2.--Values of electrical resistivity and induced polarization for natural state and resaturated samples for core samples from the USW GU-3/G-3 borehole---------- 13

Table 3.--Values of natural bulk density, saturated bulk density, dry bulk density, grain density, water-accessible porosity and compressional sonic velocity of core samples from the USW G-4 borehole---------- 22

Table 4.--Values of electrical resistivity and induced polarization for natural state and resaturated samples from the USW G-4 borehole---------- 30

Rock property measurements on large-volume core samples from Yucca Mountain USW GU-3/G-3 and USW G-4 boreholes, Nevada Test Site, Nevada

by

Lennart A. Anderson

Introduction

Core samples from the Yucca Mountain USW GU-3/G-3 and USW G-4 boreholes on Nevada Test Site (NTS) were obtained for the purpose of making rock property measurements, as part of the Nevada Nuclear Waste Storage Investigations (NNWSI) project designed to identify suitable underground repositories for radioactive waste products. Yucca Mountain lies in the southwest sector of NTS within the Topopah Spring SW Quadrangle (figure 1). Figure 1 also shows the location of the boreholes within the Yucca Mountain complex.

Core samples were selected at the drill site so as to be representative of the major lithologic variations observed within the principal stratigraphic units. Upon removal from the borehole, the cores were washed free of drilling mud, labeled as to depth and vertical attitude, wrapped in aluminum foil, and coated with beeswax in an effort to minimize the loss of natural pore water during the period prior to rock property analysis. Following delivery to the Denver laboratories of the USGS, the samples were measured for electrical resistivity, induced polarization, porosity, bulk and grain density, and compressional sonic velocity. The results of the measurements are intended for use in the interpretation of inhole and surface geophysical surveys as well as to provide a means for rock property characterization that is not normally possible with conventional borehole techniques.

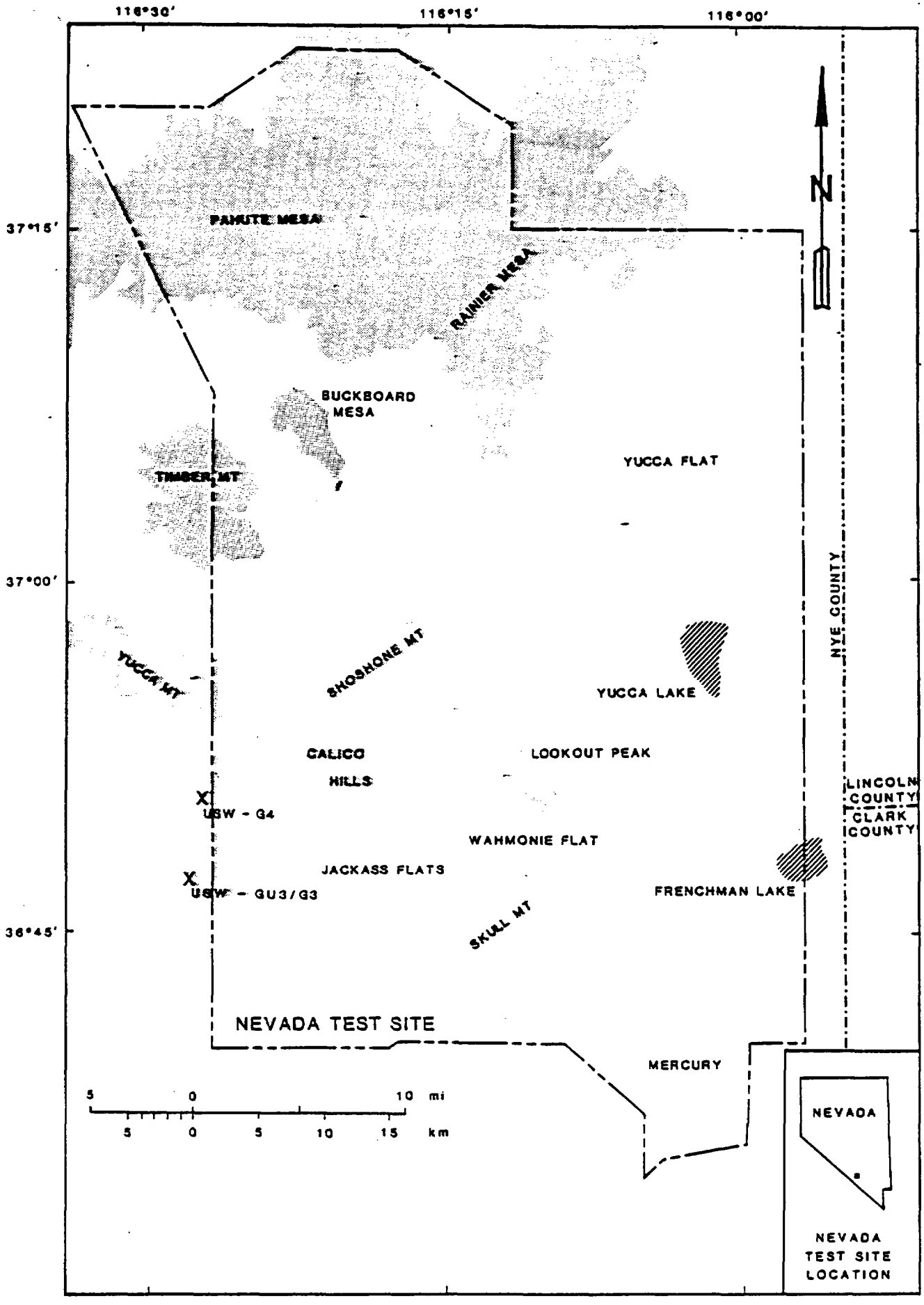

Figure 1. Map of the Nevada Test Site showing the locations of the Yucca Mountain USW GU-3/G-3 and USW G-4 boreholes.

Laboratory procedures for sample measurements

The laboratory techniques and equipment that were used to make rock property measurements have been described by Anderson (1981). Sample volumes ranged from 200 to 250 cm^3 except in the 1779.6 to 2562.4 foot (542.6-781.2 m) interval of the USW GU-3 borehole where volumes ranged from 103 to 132 cm^3.

Electrical resistivity at 100 hertz and bulk density were initially measured on "natural-state" samples. The term "natural-state" is not exact because of the likelihood that the pore water conductivity and content has been altered by drilling and handling. Hence, the measured resistivity, which varies with the conductivity and quantity of contained pore water, may differ from that of the in place rock.

After the natural-state measurements were completed the samples were dried, weighed, and then resaturated with local tap water in a partial vacuum for 72 hours. All other measurements discussed herein were made on resaturated samples.

Results of laboratory analysis of borehole USW GU-3/G-3 core samples

As the letter designation implies, USW GU-3/G-3 is actually two boreholes; G-3 being displaced approximately 100 feet (30.5 m) north-northeast of the GU-3 location. GU-3 was drilled to 2644 feet (806.1 m) and G-3 bottomed at a depth of 5031 feet (1533.8 m). Because of their close proximity, the variations observed within the respective stratigraphic units have been treated as having originated from core taken from a single continuous drillhole.

The stratigraphic sequence, lithology, and other borehole descriptions referenced in this report are taken from the work of Scott and Castellanos (1984). In descending order, the borehole penetrated the Tiva Canyon and Topopah Spring Members of the Paintbrush Tuff; the tuffaceous beds of Calico Hills (?); the Crater Flat Tuff, composed of the Prow Pass Member, the Bullfrog Member, and the Tram Member; Lithic Ridge Tuff; and older tuffs. The rocks are Miocene in age (Carr and others, 1984).

Ninety-eight core samples were taken from the listed formations which consist primarily of non-welded to densely welded ash-flows and bedded tuffs. Of those samples, one disintegrated before any measurements could be made and six others disintegrated before the full suite of measurements could be completed. Most sample losses resulted from clay expansion; others were caused by original or drill-induced fractures. Although bedded tuffs are generally the most difficult to handle, the two samples of bedded tuff in the G-3 grouping proved sufficiently competent to withstand the rigors of laboratory measurement.

Density and Porosity Measurements

Measured values of natural bulk density (NBD), saturated bulk density (SBD), dry bulk density (DBD), grain density (GD), and porosity determined by the buoyancy method (Johnson, 1979) are listed in Table 1. All density values are plotted against depth of origin in figure 2. The listed NBD values for most samples are slightly lower than the SBD values --the lower NBD values are expected for samples obtained from above the static water level (SWL). Below the SWL, at a depth of 2,640 feet or 804.9 m the NBD values are also lower than the SBD values, which suggests an occurrence of pore water loss by drainage or evaporation during sample acquisition. As indicated in Table 1, the NBD values correlate better with the SBD values than with the DBD values; the high NDB-SBD correlation indicative of a high level of saturation in the natural-state core.

In figure 2 the data points are connected with either a dashed, solid, or dotted line as an aid in following the variations in density with depth. The difference between DBD and SBD values for individual samples show the range of bulk densities possible depending upon the amount of water in the rock. Bulk density extremes for any one sample are directly related to its fractional porosity.

The formations constituting the Yucca Mountain tuffs are generally similar in mineral composition therefore the SBD and DBD variations within the sampled section are mainly caused by porosity variations. This relationship is apparent from the plots of SBD and porosity in figures 2 and 3, respectively. The densely welded tuffs of the Tiva Canyon and Topopah Spring Members of the Paintbrush Tuff might be expected to have the highest bulk densities, but the abundance of lithophysal cavities within these stratigraphic units reduces their bulk densities below those of the moderately

TABLE 1

Values of natural bulk density (NBD), saturated bulk density (SBD), dry bulk density (DBD), and grain density (GD), water-accessible porosity, and compressional sonic velocity for samples from USW GU-3/G-3 borehole.
(Leader (-) indicates no measurement possible)

sample depth in ft (m)	NBD Mg/m^3	SBD Mg/m^3	DBD Mg/m^3	GD Mg/m^3	porosity in %	Compressional sonic velocity km/s
54.2 (16.5)	2.33	2.35	2.26	2.48	9.0	4.49
96.3 (29.4)	2.32	2.32	2.20	2.50	11.7	4.40
158.8 (48.4)	2.38	2.38	2.32	2.46	5.8	4.60
207.5 (63.3)	2.38	2.38	2.33	2.45	5.1	4.70
257.0 (78.4)	2.38	2.39	2.31	2.50	7.6	4.30
305.7 (93.2)	2.36	2.38	2.30	2.49	7.9	4.31
370.9 (113.1)	1.66	1.80	1.41	2.31	38.8	2.64
435.2 (132.7)	2.22	2.29	2.12	2.56	17.3	3.08
461.1 (140.6)	2.22	2.27	2.09	2.55	18.2	3.36
552.3 (168.4)	2.27	2.28	2.14	2.49	14.2	3.96
576.0 (175.6)	1.96	2.23	2.06	2.49	17.3	4.0
610.3 (186.1)	2.26	2.28	2.13	2.49	14.3	4.16
660.3 (201.3)	2.21	2.30	2.13	2.58	17.2	3.31
713.8 (217.6)	2.36	2.39	2.30	2.53	9.0	4.33
765.0 (233.2)	2.28	2.30	2.17	2.50	13.4	3.93
825.6 (251.7)	2.41	2.41	2.35	2.52	6.8	4.51
884.1 (269.5)	2.42	2.44	2.34	2.60	10.2	4.16
925.0 (282.0)	2.32	2.36	2.25	2.53	11.2	4.05
957.7 (292.0)	2.35	2.38	2.28	2.55	10.4	4.02
1055.8 (321.9)	2.43	2.44	2.34	2.59	9.8	4.37
1108.9 (338.1)	2.42	2.43	2.35	2.56	8.3	4.43
1165.9 (355.5)	2.42	2.43	2.35	2.57	8.5	4.46
1213.2 (369.9)	2.32	2.35	2.34	2.36	1.4	4.93
1261.8 (384.7)	2.33	2.35	2.32	2.39	3.1	4.23
1310.9 (399.7)	1.88	1.94	1.65	2.32	28.7	2.43
1359.8 (414.6)	-	-	-	-	-	-
1477.2 (450.4)	1.65	1.77	1.41	2.23	36.9	1.22
1501.8 (457.9)	1.72	1.81	1.47	2.23	34.3	2.03
1566.0 (477.4)	1.62	1.74	1.30	2.31	43.6	1.28
1637.7 (499.3)	1.93	2.01	1.65	2.56	35.7	1.41
1666.7 (508.1)	1.99	2.08	1.76	2.57	31.6	1.90
1706.6 (520.3)	2.10	2.15	1.89	2.57	26.6	2.91
1779.6 (542.6)	1.58	1.84	1.45	2.40	39.7	1.41
1813.5 (552.9)	1.86	1.89	1.53	2.39	36.1	2.26
1866.9 (569.2)	2.04	1.95	1.66	2.34	29.1	2.43
1912.7 (583.1)	1.84	1.92	1.61	2.32	30.5	1.57
1958.4 (597.1)	1.83	1.89	1.55	2.36	34.3	2.23
2008.4 (612.3)	1.91	1.95	1.65	2.36	30.0	2.06
2075.0 (632.6)	2.03	2.11	1.81	2.59	29.9	2.47
2110.0 (643.3)	2.34	2.37	2.23	2.58	13.4	3.77
2167.5 (660.8)	2.26	2.30	2.12	2.58	17.7	3.09
2204.9 (672.2)	2.38	2.43	2.34	2.56	8.5	3.75

TABLE 1 - continued

2256.8 (688.0)	2.42	2.43	2.35	2.57	8.4	4.31
2315.0 (705.8)	2.42	2.44	2.36	2.58	8.4	4.30
2356.7 (718.5)	2.45	2.47	2.40	2.58	7.0	4.54
2407.2 (733.9)	2.43	2.45	2.38	2.56	7.1	4.52
2468.5 (752.6)	2.48	2.51	2.45	2.60	5.8	4.60
2521.5 (768.8)	2.36	2.39	2.29	2.54	10.1	3.89
2562.4 (781.2)	1.97	1.99	1.72	2.35	26.9	2.47
2617.5 (798.0)	2.12	2.14	1.92	2.45	21.7	2.71
2660.5 (811.1)	1.94	1.97	1.66	2.41	31.1	2.83
2730.9 (832.6)	2.05	2.10	1.79	2.58	30.7	2.52
2771.7 (845.0)	2.12	2.15	1.87	2.60	27.7	2.68
2817.7 (859.1)	2.14	2.17	1.91	2.58	25.8	2.73
2868.2 (874.5)	2.18	2.20	1.96	2.59	24.3	2.65
2913.6 (888.3)	2.29	2.31	2.13	2.60	18.0	3.34
2986.1 (910.4)	2.33	2.35	2.19	2.63	16.7	3.20
3004.1 (915.9)	2.34	2.38	2.23	2.62	14.8	3.19
3062.0 (933.5)	2.35	2.39	2.25	2.61	13.9	3.81
3115.4 (949.8)	2.34	2.36	2.23	2.56	12.8	4.12
3159.6 (963.3)	2.27	2.30	2.14	2.54	15.9	3.14
3235.0 (986.3)	2.44	2.47	2.41	2.57	6.0	4.65
3259.3 (993.7)	2.30	2.30	2.28	2.32	1.8	-
3310.7(1009.4)	2.12	2.15	1.91	2.52	24.4	3.13
3360.3(1024.5)	2.17	2.18	1.95	2.52	22.7	2.89
3411.2(1040.0)	2.13	2.18	1.95	2.52	22.3	3.0
3463.9(1056.1)	2.15	2.16	1.94	2.48	21.8	2.99
3511.2(1070.5)	2.17	2.19	1.98	2.50	20.6	3.11
3560.2(1085.4)	2.21	2.23	2.02	2.54	20.5	2.20
3611.3(1101.0)	2.26	2.28	2.12	2.52	16.2	3.38
3659.3(1115.6)	2.25	2.27	2.10	2.52	16.6	2.84
3709.9(1131.1)	2.27	2.26	2.12	2.48	14.4	1.72
3761.0(1146.6)	2.24	-	-	-	-	-
3822.7(1165.5)	2.28	2.28	2.17	2.43	10.9	3.13
3861.2(1177.2)	2.23	2.25	2.08	2.52	17.2	2.73
3912.3(1192.8)	2.21	2.22	2.02	2.51	19.5	2.78
3960.5(1207.5)	2.21	2.17	2.03	2.37	14.4	2.83
4008.9(1222.2)	2.12	2.15	1.93	2.46	21.4	2.68
4058.7(1237.4)	2.11	2.17	1.94	2.52	23.3	2.62
4110.6(1253.2)	2.19	2.20	2.03	2.45	17.0	3.42
4159.4(1268.0)	2.21	2.21	2.04	2.46	16.9	2.93
4209.5(1283.4)	2.25	2.26	2.10	2.49	15.6	2.08
4261.0(1299.1)	2.14	2.18	1.90	2.54	23.5	2.89
4311.8(1314.6)	2.17	2.20	2.02	2.46	18.0	2.84
4361.0(1329.6)	2.26	2.24	2.13	2.40	11.6	2.19
4409.9(1344.5)	2.18	2.14	1.99	2.35	15.0	2.71
4461.1(1360.1)	2.28	2.29	2.20	2.42	9.2	-
4510.8(1375.2)	2.30	2.32	2.18	2.55	14.7	-
4567.8(1392.6)	2.33	2.30	2.20	2.46	10.6	2.34
4609.6(1405.4)	2.27	2.26	2.13	2.44	13.0	-
4659.9(1420.7)	2.26	2.27	2.11	2.51	16.1	2.82
4707.9(1435.3)	2.31	2.34	2.19	2.58	15.3	2.92

TABLE 1 - continued

4755.9(1450.0)	2.26	2.28	2.10	2.56	17.9	2.25
4818.6(1469.1)	2.22	2.24	2.05	2.53	19.3	3.06
4860.8(1482.0)	2.22	2.23	2.06	2.50	17.5	3.32
4910.7(1497.2)	2.24	2.25	2.10	2.46	14.6	2.65
4977.9(1517.7)	2.26	2.23	2.09	2.43	13.8	2.77
5009.8(1527.4)	2.32	2.34	2.22	2.54	12.6	3.87

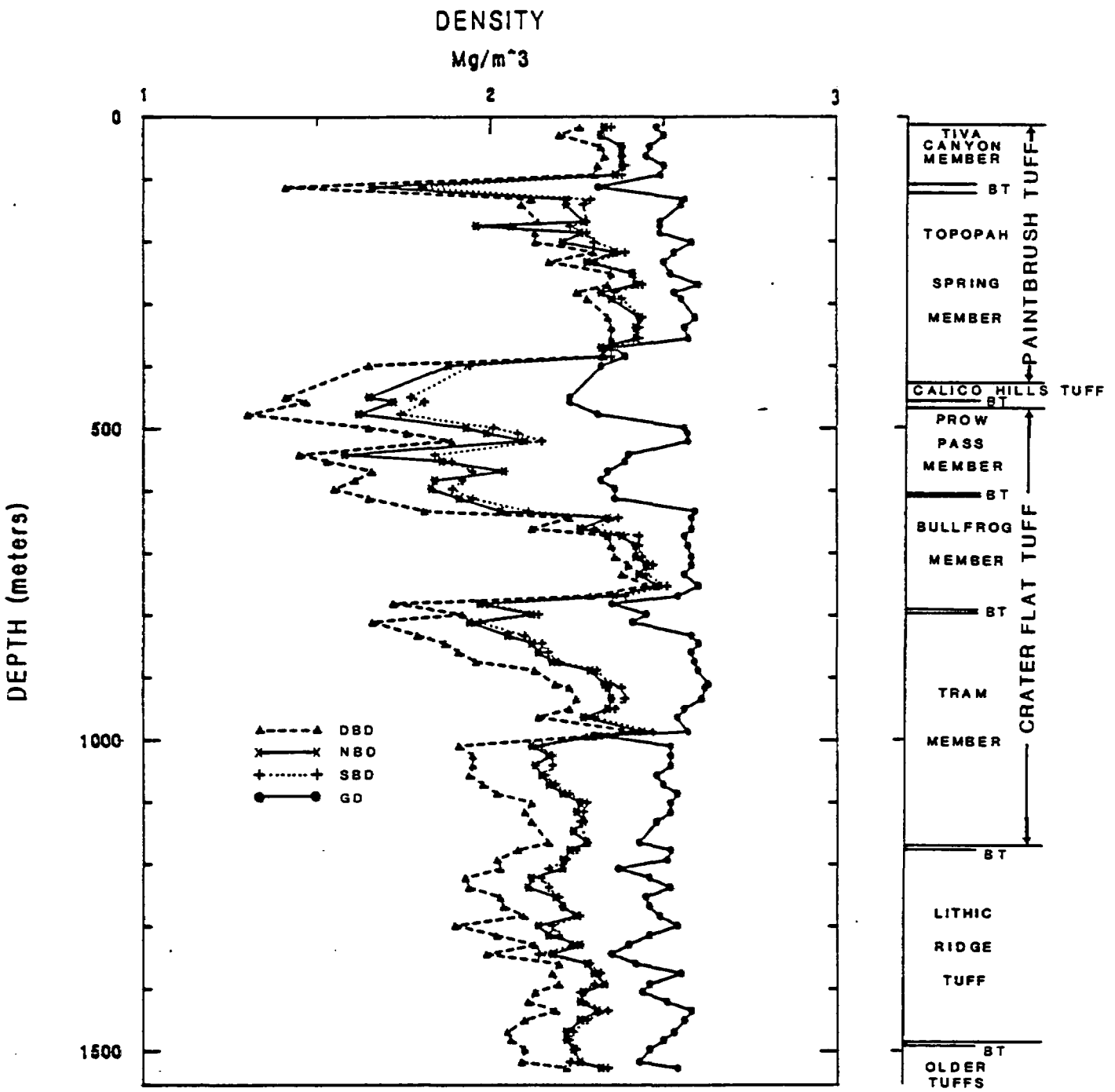

Figure 2. Density values for USW GU-3/G-3 core samples plotted as a function of depth of origin. DBD is dry bulk density; NBD is natural bulk density; SBD is saturated bulk density; and GD is grain density. BT in the stratigraphic column refers to bedded tuff.

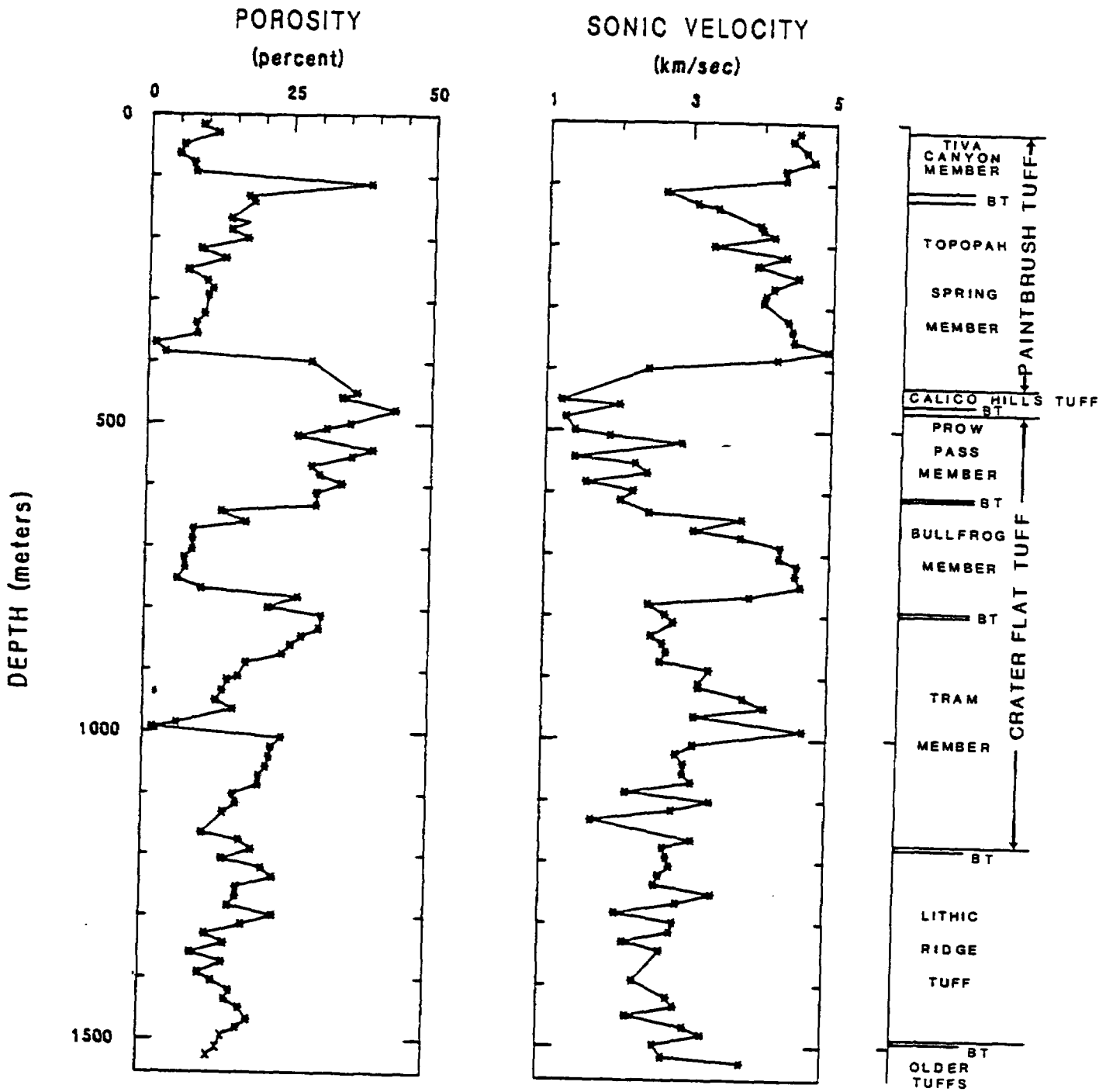

Figure 3. Porosity and compressional sonic velocity values for USW GU-3/G-3 core samples plotted as a function of depth of origin.

to densely welded Bullfrog member of the Crater Flat Tuff. Mineral alteration, pumice, lithic fragments, and phenocrysts of a large variety of minerals alter the density of many samples, obscuring and disrupting any direct correspondence between SBD and porosity.

The grain densities (GD) values plotted in figure 2 are believed to vary primarily with pumice content. Pumice has a much lower measured GD in its bulk form than in its powdered form owing to its occluded pore spaces. As a result, rock which contains pumice has a lower bulk density than its mineral composition would normally predict. Compaction and flattening of glassy components which normally accompanies welding, eliminates the variability in grain density such that densely welded zones can easily be distinguished from nonwelded zones by means of borehole density logs.

Compressional Sonic Velocity

Porosities and compressional sonic velocities of the G-3 saturated core samples are listed in Table 1 and are plotted in figure 3. The sonic travel path was along the axis of the core as mounted in the sample holder under moderate uniaxial pressure. Thus, the values shown are relative velocities and do not take into account the effect of increasing lithostatic pressure with depth.

For a rock of given composition sonic velocity is primarily dependent upon porosity. The inverse correlation between porosity and sonic velocity shown in figure 3 is not precise inasmuch as other physical characteristics of the rock such as texture, fractures, and fracture-filling minerals also affect sonic velocity. The high-velocity, low-porosity, densely-welded tuffs of the Paintbrush Tuff and Bullfrog Member of the Crater Flat Tuff have the most uniform lithology. In contrast, the Tram Member of the Crater Flat Tuff and Lithic Ridge Tuff have a less obvious correlation between velocity and

porosity, which is attributed to large lithic fragments and a high percentage of phenocrysts of feldspar and quartz in the groundmass.

Electrical measurements

Resistivity and induced polarization measurements made on the G-3 samples are listed in Table 2. A plot comparing 100 hertz resistivity of natural state versus resaturated samples is shown in figure 4. As previously mentioned, the NBD and SBD values of the Tiva Canyon tuff samples are similar; where differences occur the NBD values are always low, indicating a slight loss of pore water. In all cases, however, the pore water content is very nearly the same before and after resaturation.

TABLE 2

Values of electrical resistivity and induced polarization for natural state and resaturated samples for core samples from the USW GU-3/G-3 borehole
(Leader (-) indicates no measurement possible)

Sample depth ft (m)	100 Hz resistivity in ohm-m natural state	100 Hz resistivity in ohm-m resaturated	dc resistivity in ohm-m (resaturated)	Induced polarization in %	Specific capacity x 10^8 in farads/m
54.2 (16.6)	6345	7276	7954	8.6	32
96.3 (29.4)	3295	3925	4389	7.6	52
158.8 (48.4)	6630	7492	8262	5.2	19
207.5 (63.3)	6065	6910	7476	4.7	19
257.0 (78.4)	4370	4848	5124	4.6	27
305.7 (93.2)	2285	2787	-	-	-
370.9 (113.1)	50	51	58	9.8	5070
435.2 (132.7)	1350	997	964	4.0	125
461.1 (140.6)	1230	851	836	4.7	169
552.3 (168.4)	645	629	689	5.6	244
576.0 (175.6)	1065	966	959	4.2	131
610.3 (186.1)	885	781	772	4.5	175
660.3 (201.3)	445	470	468	5.1	327
713.8 (217.6)	1315	1392	1389	4.4	95
765.0 (233.2)	580	561	608	5.5	271
825.6 (251.7)	1430	1294	1440	3.0	63
884.1 (269.5)	634	772	802	5.6	209
925.0 (282.0)	830	717	830	5.4	195
957.7 (292.0)	805	664	745	5.8	233
1055.8(321.9)	7055	6123	6744	8.1	36
1108.9(338.1)	1765	1800	1929	5.8	90
1165.9(355.5)	1760	1684	1889	5.3	84
1213.2(369.9)	785	1161	967	2.9	90
1261.8(384.7)	3315	3180	3634	6.1	50
1310.9(399.7)	205	191	180	4.4	733
1359.8(414.6)	-	-	-	-	-
1477.2(450.4)	145	156	163	4.1	755
1501.8(457.9)	142	123	118	4.8	1220
1566.0(477.4)	80	84	76	3.4	1342
1637.7(499.3)	105	97	81	1.5	556
1666.7(508.1)	145	138	165	4.2	764
1706.6(520.3)	210	219	194	5.4	835
1779.6(542.6)	60	56	65	9.5	4385
1813.5(552.9)	120	87	107	8.1	2271
1866.9(569.2)	70	60	69	5.3	2304
1912.7(583.1)	45	43	53	5.3	3000
1958.4(597.1)	50	45	54	6.4	3556
2008.4(612.3)	30	32	39	4.3	3308
2075.0(632.6)	155	130	174	9.0	1551

TABLE 2 - continued

2110.0(643.3)	690	526	663	6.1	276
2167.5(660.8)	295	232	281	7.5	800
2204.9(672.2)	800	689	810	6.8	252
2256.8(688.0)	655	650	797	5.1	192
2315.0(705.8)	960	823	1010	5.5	163
2356.7(718.5)	1525	1505	1861	5.0	81
2407.2(733.9)	1260	1212	1226	5.8	142
2468.5(752.6)	3175	3181	3900	5.2	40
2521.5(768.8)	800	787	976	5.0	154
2562.4(781.2)	145	130	148	3.9	790
2617.5(798.0)	40	39	46	3.0	1957
2660.5(811.1)	50	61	64	6.6	3094
2730.9(832.6)	120	126	145	6.2	1283
2771.7(845.0)	135	145	165	5.4	982
2817.7(859.1)	111	125	142	5.8	1225
2868.2(874.5)	155	168	199	4.6	693
2913.6(888.3)	232	225	261	4.7	540
2986.1(910.4)	530	495	592	6.5	329
3004.1(915.9)	691	633	741	4.1	166
3062.0(933.5)	811	752	842	4.1	146
3115.4(949.8)	370	404	481	4.9	306
3159.6(963.3)	230	255	305	6.4	630
3235.0(986.3)	865	1200	1366	3.4	75
3259.3(993.7)	32	-	-	-	-
3310.7(1009.4)	77	81	102	7.0	2059
3360.3(1024.5)	40	39	48	5.0	3125
3411.2(1040.0)	50	47	56	4.3	2304
3463.9(1056.1)	55	53	63	4.2	2000
3511.2(1070.5)	55	54	65	3.0	1385
3560.2(1085.4)	40	44	55	2.7	1473
3611.3(1101.0)	60	62	71	2.1	887
3659.3(1115.6)	35	37	42	1.8	1286
3709.9(1131.1)	25	23	25	2.0	2400
3761.0(1146.6)	15	-	-	-	-
3822.7(1165.5)	35	38	48	5.9	3688
3861.2(1177.2)	50	60	71	3.2	1352
3912.3(1192.8)	40	45	51	4.1	2412
3960.5(1207.5)	50	54	69	8.6	3739
4008.9(1222.2)	35	39	48	8.2	5125
4058.7(1237.4)	60	68	80	8.2	3075
4110.6(1253.2)	80	98	128	8.8	2063
4159.0(1268.0)	51	56	75	9.9	3960
4209.5(1283.4)	35	42	49	5.1	3122
4261.0(1299.1)	78	90	104	9.6	2769
4311.8(1314.6)	35	44	50	4.6	2760
4361.0(1329.6)	15	16	16	2.1	3938
4409.9(1344.5)	35	44	51	4.4	2588
4461.1(1360.1)	11	-	-	-	-
4510.8(1375.2)	15	-	-	-	-

TABLE 2 - continued

4567.8(1392.6)	27	26	27	2.0	2222
4609.6(1405.4)	22	-	-	-	-
4659.9(1420.7)	37	38	52	6.0	3462
4707.9(1435.3)	48	52	68	4.1	1809
4755.9(1450.0)	33	49	55	4.9	2673
4818.6(1469.1)	79	101	133	9.2	2075
4860.8(1482.0)	37	42	53	5.2	2943
4910.7(1497.2)	64	66	79	4.1	1557
4977.9(1517.7)	18	21	24	2.8	3500
5009.8(1527.4)	130	131	151	3.9	775

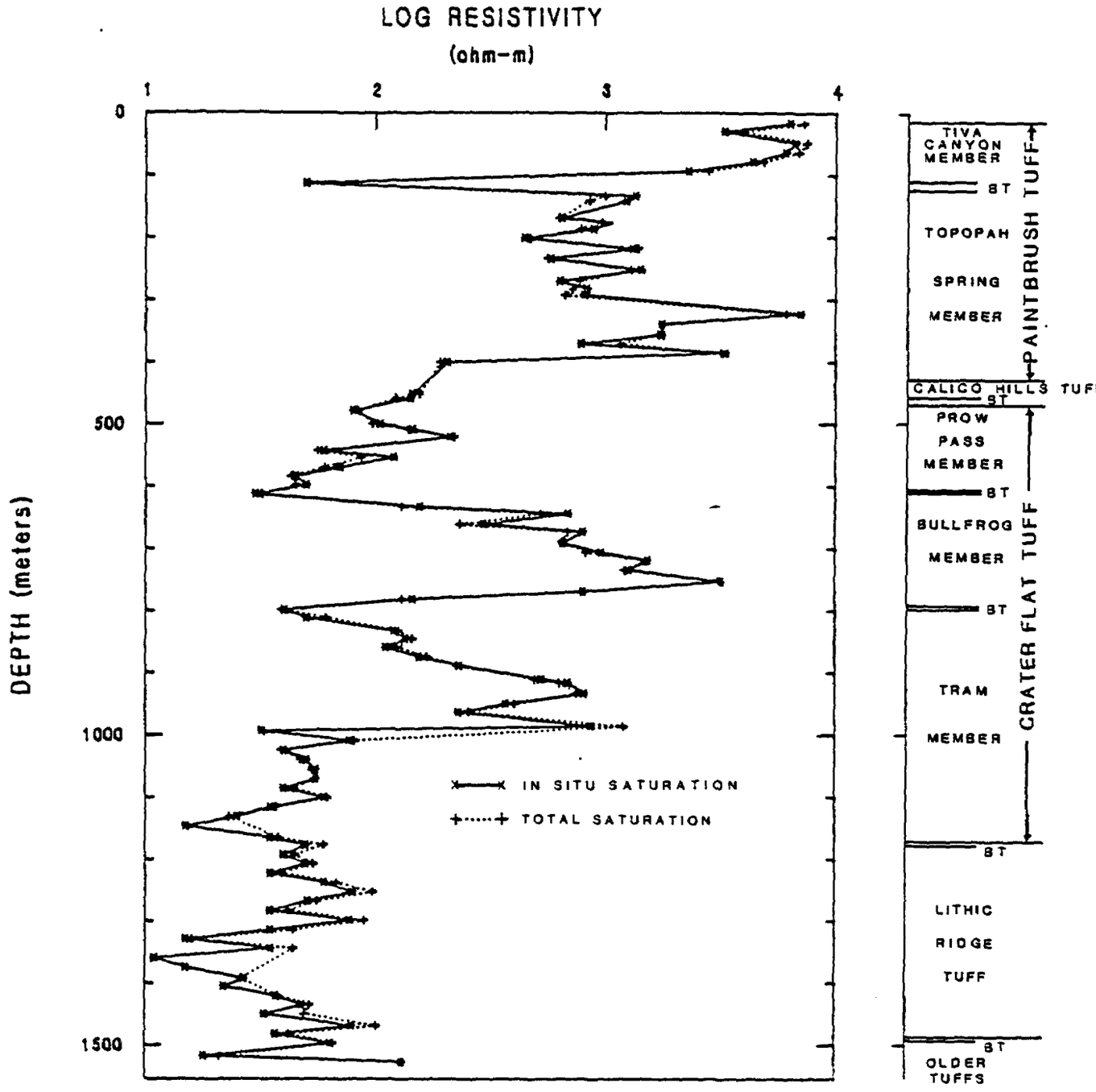

Figure 4. Resistivity values for USW GU-3/G-3 natural state and resaturated core samples plotted against depth of origin.

Resistivities of the resaturated samples are significantly higher for all Tiva Canyon samples which indicates that the pore water resistivity in the natural state is lower than that of the water used for resaturation. Local tap water has a resistivity of 14.5 ohm-m at 22° C.

The Topopah Spring Member is represented is by samples in the 435-1360 foot (132.6-414.6 m) interval. These samples show a different, but sometimes inconsistent, pattern of resistivities. Generally, the resistivities of the resaturated rocks are lower than the values under natural state conditions as may be expected for samples taken from above the static water level. Out of 18 Topopah Spring tuff samples measured, 5 show higher resistivities following resaturation but in 4 of the 5 cases the resistivity values in both the natural and resaturated states are, within the limits of measurement accuracy, very nearly the same.

With few exceptions, the Crater Flat Tuff samples from both above and below the water table have saturated resistivity values lower than, or about equal to, the natural-state resistivities. The natural-state resistivities of the Lithic Ridge Tuff and older tuff samples are generally lower than the resaturated resistivity values. For these lower units the in place pore water resistivity is apparently less than the resistivity of the Denver tap water used in the resaturation process.

Resistivity and induced polarization values obtained simultaneously on resaturated samples at a frequency of 0.125 Hz are listed in Table 2. Typically the dc resistivities are slightly higher than those measured at 100 Hz because of the frequency dependence of the dielectric constant of the rock. In some instances the dc resistivities are lower than those of the 100 Hz measurement, possibly as the result of a longer soaking period and consequently a higher level of saturation. The resistivity differences

between the three sets of measurements are not considered to be significant as the character of the resistivity variation is preserved in each individual data set.

Measurements of induced polarization (IP) were made in the time domain. The transient decay voltage, integrated over a 30 msec time interval, was normalized by the primary voltage and the IP effect read directly from the measuring instrument as a dimensionless quantity or in terms of percent. The IP values plotted in figure 5 are in the range typical of clay bearing rocks. Although there are high and low points on the plot, the IP data in itself are not always definitive in outlining the zones of greatest clay and zeolite mineral concentrations. Porosity changes (as indicated by resistivity variations) play an important part in controlling current distribution through the rock. Hence, low porosity rock with relatively few conduction paths concentrates current flow to the extent that the polarization effect is greatly enhanced. As a result, low volumes of polarizable materials may produce an IP response equal to that observed in a clay-rich, high porosity rock. Examples of such occurrences can be seen in the Paintbrush Tuff sample group. The sample from the 54.2 foot (16.6m) level is a high resistivity, densely welded tuff reportedly containing no polarizable materials except for some hematite within the mineral linings of lithophysal cavities found in the Tiva Canyon interval. The 370.9 foot (113.1m) is a non-welded tuff whose groundmass has been altered to clay (smectite), which partially accounts for its low resistivity. Both samples have approximately the same IP response, despite their widely differing clay content. A procedure sometimes followed in the mining industry to obtain a better estimate of the quantity of polarizable material within the rock is to compute the ratio of the IP and

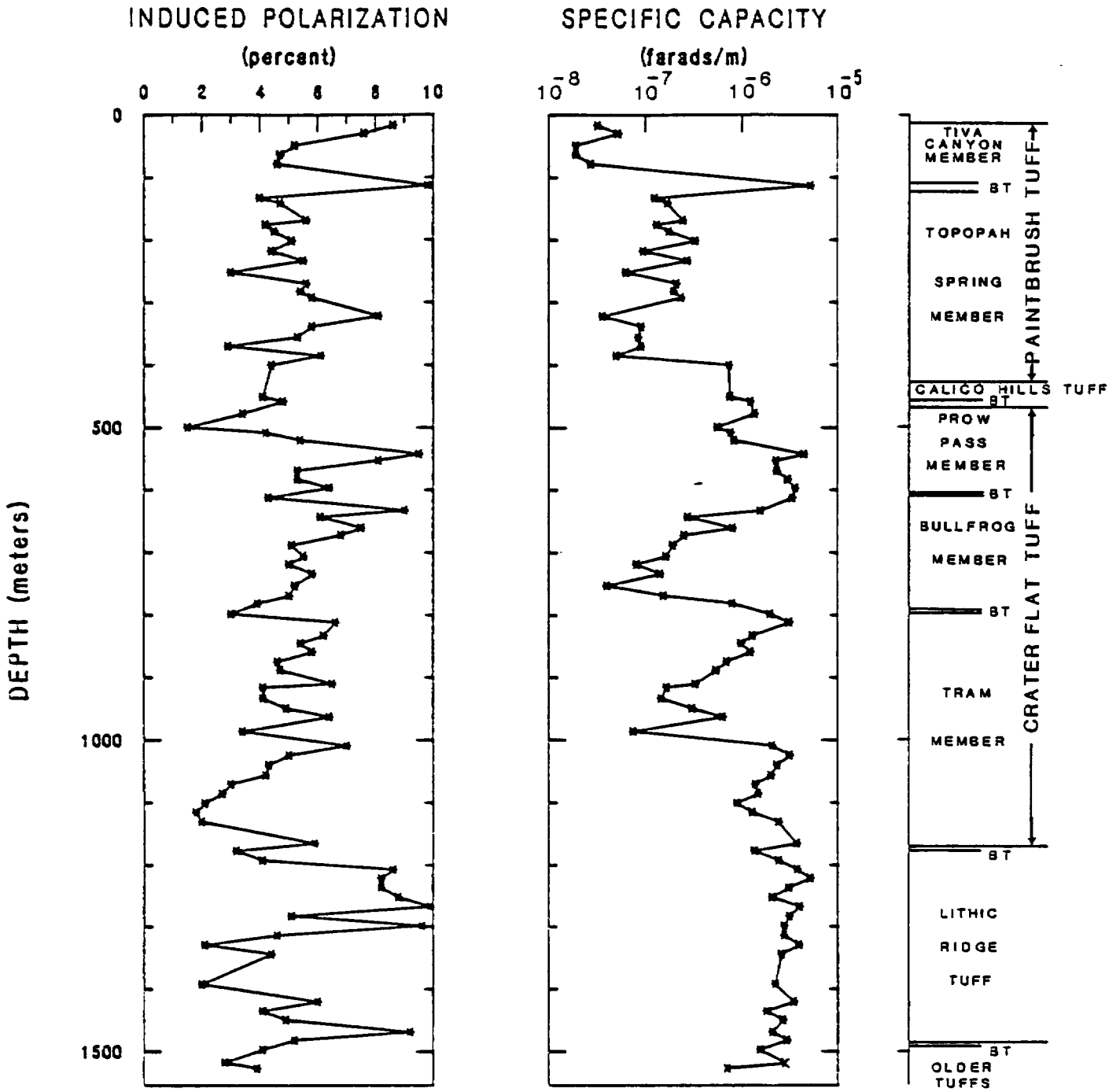

Figure 5. Induced polarization values for USW GU-3/G-3 core samples plotted against depth of origin. Induced polarization is expressed in terms of percent and in specific capacity in farads/m.

resistivity data (Sumner, 1976). As indicated, the Huntec MK III receiver used in the IP measurement presents induced polarization as the ratio of the secondary and primary voltage (Vs/Vp). In the time domain this dimensionless quantity can be converted to specific capacity, χ, using the equation

$$\chi = [(Vs \times Tp)/(Vp \times \rho)]$$

where Tp is the secondary voltage integrating time, which in this instance is 30 milliseconds, and ρ is the resistivity. The unit for specific capacity is farads/m.

The χ values are listed in Table 2 and also plotted in figure 5. As reported by Madden and Marshall (1959), specific capacity — or its frequency-domain equivalent "metal factor" — is useful in estimating quantities of polarizable materials in igneous rock, but, in poorly consolidated rock such as non-welded tuff, the increase in the number of conduction paths tends to diminish the diagnostic qualities of the parameter. Despite this limitation, specific capacity values are useful as an indicator of clay and zeolite concentrations. Figure 4 shows the Crater Flat Tuff, and, in particular, the Lithic Ridge Tuff to be host to the highest amounts of polarizable minerals, including pyrite in the 3878.9-4021.3 foot (1182.6-1226.0m) interval.

Results of laboratory analysis of Borehole USW G-4 core samples

The stratigraphy, lithology, and miscellaneous details pertaining to borehole USW G-4 have been described by R. W. Spengler (written commun., 1982). Drilling was completed at a depth of 3001 feet (914.7m) penetrating the Tiva Canyon, Pah Canyon, and Topopah Spring Members of the Paintbrush Tuff; the tuffaceous beds of Calico Hills; the Prow Pass and Bullfrog Members of the Crater Flat Tuff; and the upper section of the Tram Member, also of the Crater Flat Tuff. A very thin section of the Yucca Mountain Member of the Paintbrush Tuff was identified but was not sampled. Several bedded tuff intervals exist within the drilled section but no samples from these units were obtained because of the difficulty in maintaining a shaped sample taken from a core of poorly consolidated ash. In total, 46 samples were taken from the available core and measured as described for the GU-3/G-3 sample units.

Density and Porosity

Bulk and grain density values obtained on the G-4 core are listed in Table 3 and plotted versus depth of origin in figure 6. The NBD values above and below the 1776 foot (542.5m) static water level are equal to or slightly lower than the SBD values, which indicates some loss of pore water following removal of the core from the borehole. NBD-SBD differences are greatest in the 280 to 603 foot (85.4-183.8m) interval — this zone may be undersaturated in its natural setting.

TABLE 3

Values of natural bulk density (NBD), saturated bulk density (SBD), dry bulk density (DBD), grain density (GD), water-accessible porosity, and compressional sonic velocity of core samples from the USW G-4 borehole.

Sample depth in ft (m)	NBD Mg/m^3	SBD Mg/m^3	DBD Mg/m^3	GD Mg/m^3	Porosity in %	Compressional sonic velocity km/s
59.0 (18.0)	2.41	2.42	2.37	2.51	5.5	4.68
90.8 (27.7)	2.35	2.37	2.29	2.49	8.0	4.34
169.6 (51.7)	1.42	1.68	1.16	2.41	51.9	1.97
280.4 (85.5)	2.28	2.37	2.23	2.57	13.0	2.84
332.3(101.3)	2.23	2.32	2.16	2.56	15.7	3.66
390.3(119.0)	2.27	2.34	2.21	2.54	12.9	3.01
548.4(167.2)	2.05	2.21	2.00	2.51	20.3	4.05
602.6(183.7)	2.18	2.28	2.11	2.54	16.8	4.24
668.6(203.8)	2.35	2.35	2.23	2.53	11.9	4.36
742.5(226.4)	2.37	2.39	2.31	2.50	7.4	4.58
821.2(250.4)	2.35	2.36	2.24	2.53	11.5	4.36
875.5(266.9)	2.41	2.43	2.33	2.58	9.9	4.59
937.6(285.9)	2.38	2.39	2.28	2.56	10.8	4.43
1064.5(324.5)	2.30	2.33	2.19	2.55	13.8	4.31
1239.2(377.8)	2.40	2.44	2.34	2.59	9.4	4.65
1361.5(415.1)	2.09	2.14	1.97	2.37	16.9	3.85
1431.5(436.4)	1.84	1.84	1.47	2.32	36.6	2.24
1468.2(447.6)	1.89	1.86	1.54	2.27	32.1	2.14
1511.4(460.8)	1.92	1.91	1.59	2.34	31.8	2.92
1570.3(478.8)	1.85	1.84	1.48	2.31	35.8	1.88
1627.2(496.1)	1.89	1.90	1.57	2.33	32.6	2.38
1678.4(511.7)	1.90	1.91	1.56	2.38	34.3	2.82
1784.3(544.0)	1.96	1.95	1.66	2.36	29.7	2.43
1822.8(555.7)	2.01	2.05	1.71	2.61	34.6	2.40
1870.7(570.3)	2.10	2.13	1.83	2.61	29.8	2.53
1915.8(584.1)	2.24	2.26	2.06	2.56	19.4	3.59
1976.0(602.4)	1.96	1.97	2.64	2.43	32.5	2.45
2032.4(619.6)	1.94	1.96	1.61	2.47	35.0	1.75
2072.9(632.0)	2.10	2.10	1.89	2.38	20.6	2.43
2131.2(649.8)	2.06	2.06	1.82	2.40	24.3	2.97
2181.8(665.2)	1.98	1.99	1.70	2.40	29.2	3.08
2228.5(679.4)	2.00	1.99	1.71	2.39	28.6	2.24
2298.0(700.6)	2.17	2.18	1.93	2.57	24.8	2.98
2336.8(712.4)	2.18	2.19	1.94	2.57	24.4	2.96
2381.6(726.1)	2.26	2.27	2.06	2.60	20.8	3.53
2436.1(742.7)	2.19	2.20	1.95	2.62	25.7	3.10
2478.0(755.5)	2.19	2.21	1.96	2.62	25.0	2.97
2523.7(769.4)	2.22	2.23	2.01	2.57	21.9	2.96
2577.7(785.9)	2.32	2.33	2.15	2.62	18.2	3.95
2637.5(804.1)	2.41	2.42	2.31	2.60	11.3	4.28

TABLE 3 - continued

2694.6(821.5)	2.05	2.05	1.77	2.46	28.0	2.85
2719.5(829.1)	2.01	2.02	1.77	2.37	24.7	3.32
2826.2(861.7)	2.04	2.04	1.76	2.44	27.6	3.00
2856.8(871.0)	2.27	2.27	2.08	2.58	19.6	3.81
2938.6(895.9)	2.28	2.29	2.10	2.59	18.9	3.96
2979.8(908.5)	2.34	2.36	2.20	2.60	15.2	4.05

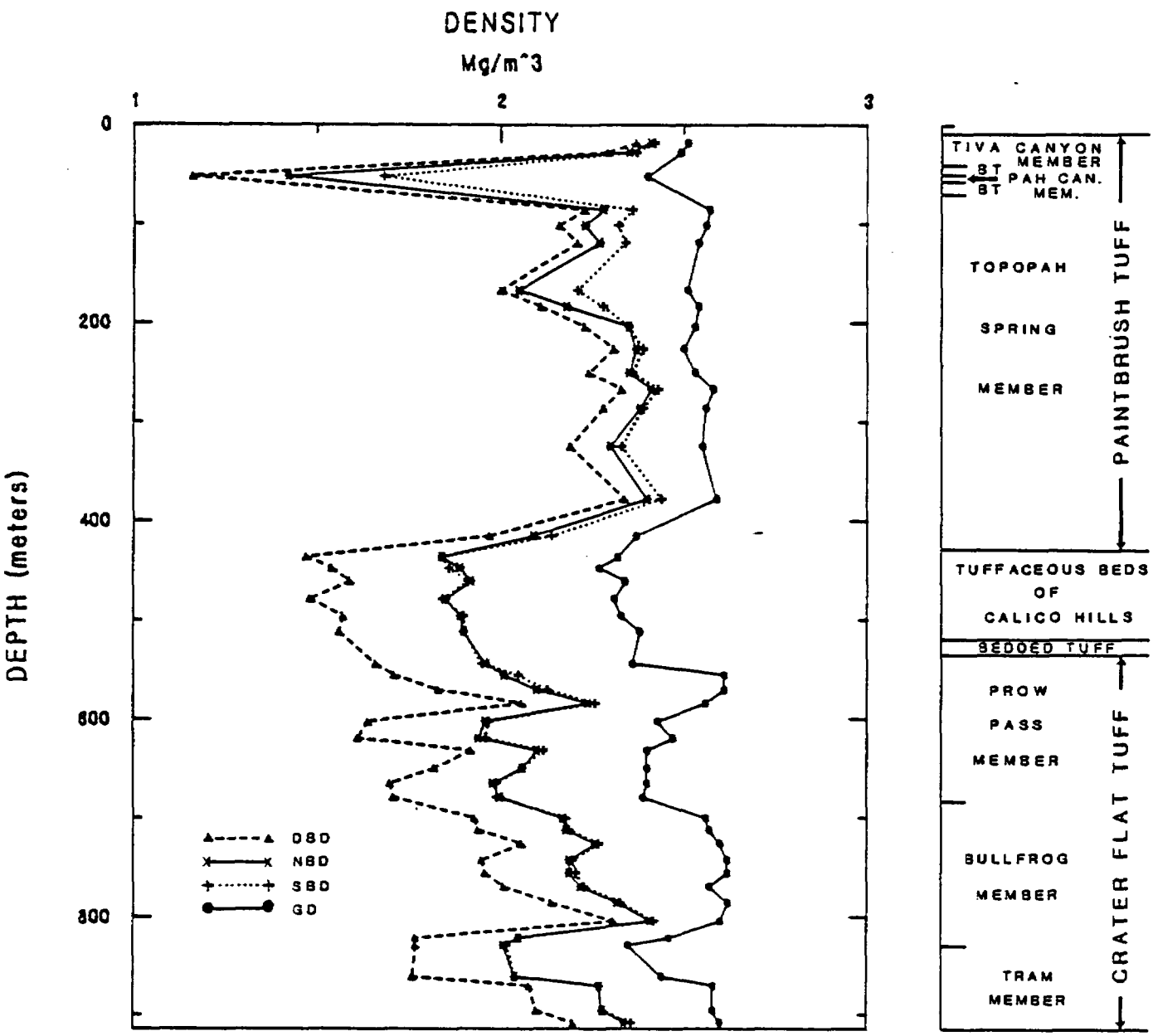

Figure 6. Density values for USW G-4 core samples plotted against depth of origin. DBD, NBD, SBD, and GD are as indicated in Figure 2. BT is the stratigraphic column refers to bedded tuff.

Variations in bulk density (figure 6) are primarily the result of porosity changes and pumice content, and, to a lesser degree, fractures, alteration products, and accessory minerals. Except for its lower, non-welded section, the Topopah Spring Member of the Paintbrush Tuff is the most uniform in bulk density. Bulk densities are somewhat lower in the upper section of the Topopah Spring Member because of the occurrence of lithophysal cavities in that zone. At greater depth, the bulk densities of the formations are much more variable; the highest densities associated with intervals of densely welded tuff.

Grain density changes usually signify differences in mineral composition between samples. However, the mineral composition of the Yucca Mountain Tuffs is reasonably uniform, therefore the main GD variations observed in figure 6 must stem from the condition of the pumice fragments within the rock. In non-welded tuff the intergranular pore spaces of the pumice are effectively sealed. As a result, GD determinations made by the water saturation method produce lower values than would be predicted from the mineral constituents which make up the rock. In welded tuffs the pumice fragments have collapsed thereby destroying their internal pore structure. Measured GD values of welded tuff therefore approximate the true GD of the mineral constituents of the rock.

Grain densities are highest in the welded zones of the Crater Flat Tuff because of a greater concentration of phenocrysts within the groundmass. The phenocrysts consist primarily of quartz, sanidine, plagioclase, hornblende, and biotite which have GD values in the 2.6-3.2 Mg/m^3 range.

Porosity values are listed in Table 3 and plotted against depth of origin in figure 7. The lowest porosities are associated with the densely welded

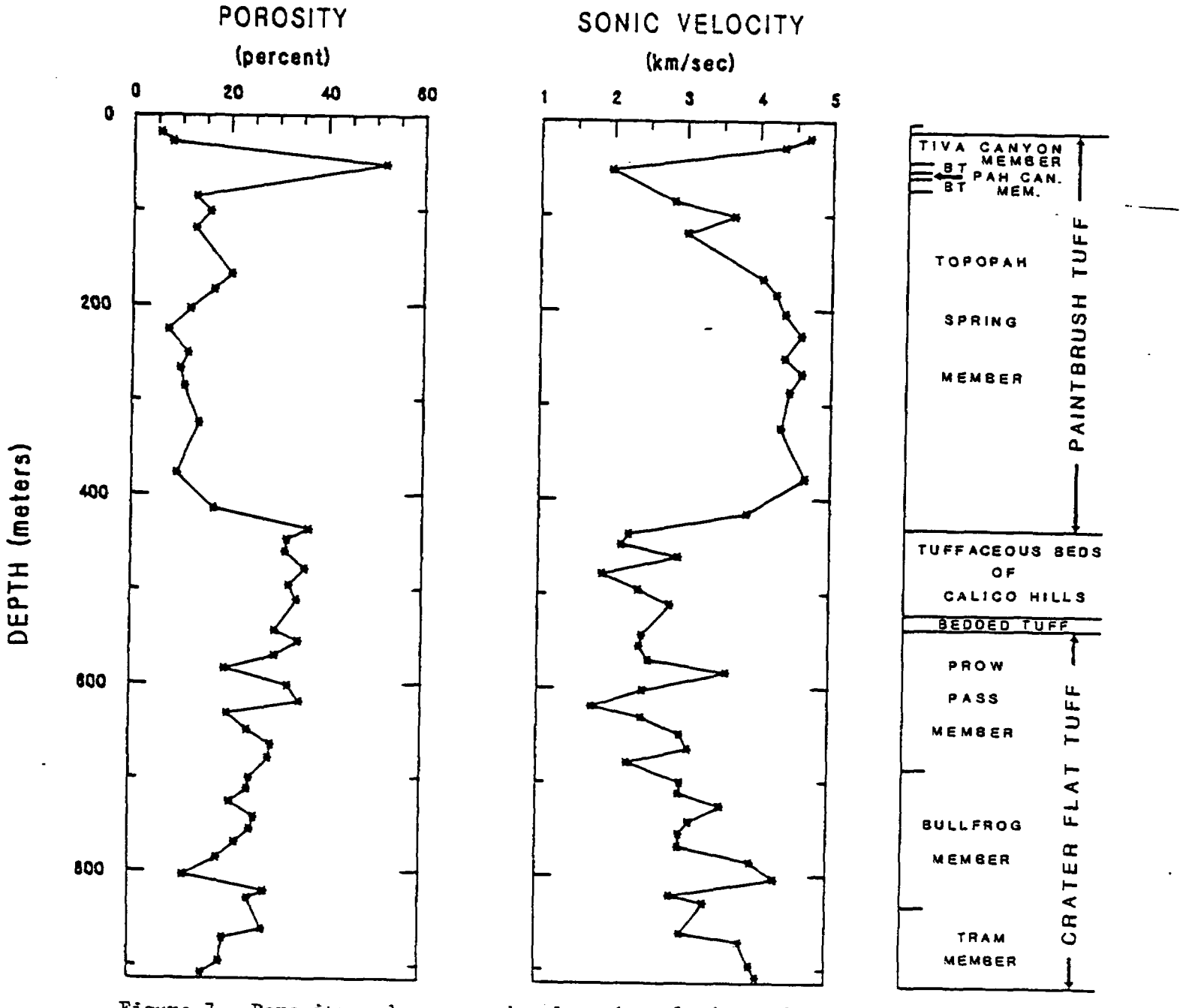

Figure 7. Porosity and compressional sonic velocity values for USW G-4 core samples plotted as function of depth of origin.

tuffs of the Tiva Canyon and Topopah Spring Members of the Paintbrush Tuff. At greater depth the tuffaceous beds of Calico Hills and Crater Flat Tuff have porosities generally in excess of 20 percent. Individual units of the Crater Flat Tuff have highly variable porosities indicating a high variability in the level of welding within any one unit.

Compressional Sonic Velocity

As discussed in the section pertaining to sonic velocity data of the GU-3/G-3 samples, there are certain physical factors in the makeup of a rock which have an effect on the propagation velocity of an acoustical pulse as it moves through the sample. However, the principal rock property controlling sonic velocity is porosity as can be seen in the inverse relationship between the porosity and sonic velocity plots in figure 7. The sonic velocity shows the Topopah Spring Member to be most uniformly compacted section encountered within the G-4 borehole.

Electrical Measurements

The results of resistivity and induced polarization measurements on the G-4 borehole samples are listed in Table 4. Figure 8 is a plot of natural state and resaturated sample resistivities made at 100 hertz. For the most part the resaturated samples are somewhat lower than the natural state resistivities. Exceptions exist for samples from the Tuffaceous Beds of Calico Hills. In this section, bulk density measurements indicate the natural state samples to be undersaturated, yet the natural state resistivities are consistently lower than the sample resistivities following resaturation. Apparently the conductivity of the in place pore waters is appreciably higher than the conductivity of the water used for resaturation. It is also possible that ions contained in the pore waters of these high porosity rocks diffused into the surrounding water bath following the saturation process so as to

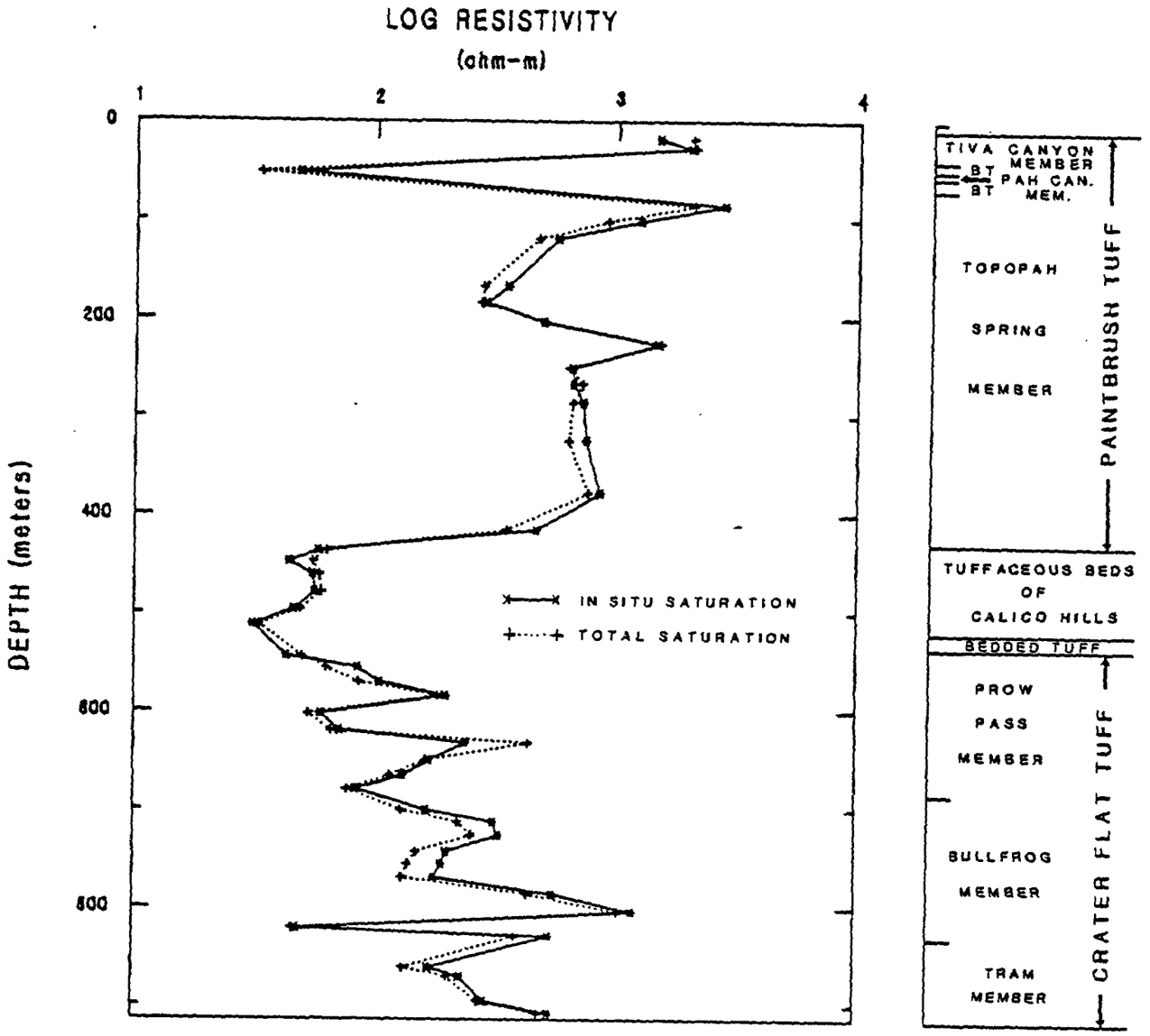

Figure 8. Resistivity values for USW G-4 natural state and resaturated core samples plotted against depth of origin.

increase the pore water resistivity of the resaturated samples. The tuffs of the Crater Flat Tuff are very similar to the Calico Hills tuffs but, according to Spengler (written commun., 1982), contain greater quantities of clays and zeolites. The result is high surface conduction, which diminishes the sensitivity of the bulk resistivity to small changes in the resistivity of the contained pore water.

The IP plot in Figure 9 shows small deviations from a background level of from four to six percent. To enhance the informational content of the IP data, the individual values were converted to specific capacity in the same manner as has been described for the G-3 borehole IP data. The highest value is associated with the Pah Canyon Member which is a clay-rich, non-welded, high porosity section. High specific capacity values are observed over the entire Calico Hills tuff interval. Although the Crater Flat Tuff samples are more zeolitized, their specific capacities are much more variable and do not reach the high level attained by the Calico Hills tuffs. Changes in both degree of welding and levels of silicification are the likely causes of the variability in the specific capacity data. In porous rock much of the current flow is through the pore waters, with little surface conduction due to clays and zeolites. Low resistivities are typically the result, accompanied by a relatively low IP response. However, normalizing the IP effect by the resistivity of the rock produces higher specific capacity values than warranted for the amount of polarizable material present. Hence, the amplitude of the specific capacity can not be relied upon as an indicator of the quantity of clays or zeolites within the rock.

TABLE 4

Values of electrical resistivity and induced polarization for natural state and resaturated samples from the USW G-4 borehole.

Sample depth in ft (m)	100 Hz resistivity in ohm-m natural state	100 Hz resistivity in ohm-m resaturated	dc resistivity in ohm-m (saturated)	Induced polarization in %	Specific capacity x 10^8 in farads/m
59.0 (18.0)	1489	2049	2186	4.1	56
90.8 (27.7)	2007	2105	2280	3.6	47
169.6 (51.7)	48	33	40	10.2	7650
280.4 (85.5)	2762	2066	2136	4.3	60
332.3(101.3)	1244	912	943	4.9	156
390.3(119.0	565	469	520	6.3	363
548.4(167.2)	351	278	319	6.6	621
602.6(183.7)	285	271	315	5.8	552
668.6(203.8)	494	502	558	5.6	301
742.5(226.4)	1472	1526	1638	4.4	81
821.2(250.4)	654	634	712	5.4	228
875.5(266.9)	661	724	789	6.2	236
937.6(285.9)	729	656	721	5.0	208
1064.5(324.5)	746	632	704	5.4	230
1239.2(377.8)	856	765	825	5.1	185
1361.5(415.1)	465	350	416	8.8	635
1431.5(436.4)	58	63	69	6.6	2870
1468.2(447.6)	44	55	60	4.8	2400
1511.4(460.8)	55	59	64	4.2	1969
1570.3(478.8)	56	60	66	5.9	2682
1627.2(496.1)	46	49	54	4.0	2222
1678.4(511.7)	31	33	37	3.6	2919
1784.3(544.0)	43	50	52	3.9	2250
1822.8(555.7)	85	63	70	7.0	3000
1870.7(570.3)	105	86	92	5.0	1630
1915.8(584.1)	198	184	202	4.3	639
1976.0(602.4)	60	53	59	4.9	2492
2032.4(619.6)	72	66	72	5.2	2167
2072.9(632.0)	239	436	661	3.9	177
2131.2(649.8)	169	163	170	2.9	512
2181.8(665.2)	132	116	129	6.0	1395
2228.5(679.4)	84	77	84	3.1	1107
2298.0(700.6)	165	130	146	6.7	1377
2336.8(712.4)	314	224	231	4.8	623
2381.6(726.1)	330	255	279	6.0	645
2436.1(742.7)	200	150	153	5.2	1020
2478.0(755.5)	191	138	144	6.0	1250
2523.7(769.4)	178	131	143	7.4	1552
2577.7(785.9)	556	436	474	3.7	234
2637.5(804.1)	1186	1035	1112	3.8	103
2694.6(821.5)	48	46	49	2.2	1347

TABLE 4 - continued

2719.5(829.1)	537	388	434	6.0	415
2826.2(861.7)	170	133	143	4.9	1028
2856.8(871.0)	231	204	225	4.7	627
2938.6(895.9)	291	274	301	4.7	468
2979.8(908.5)	540	486	538	4.8	268

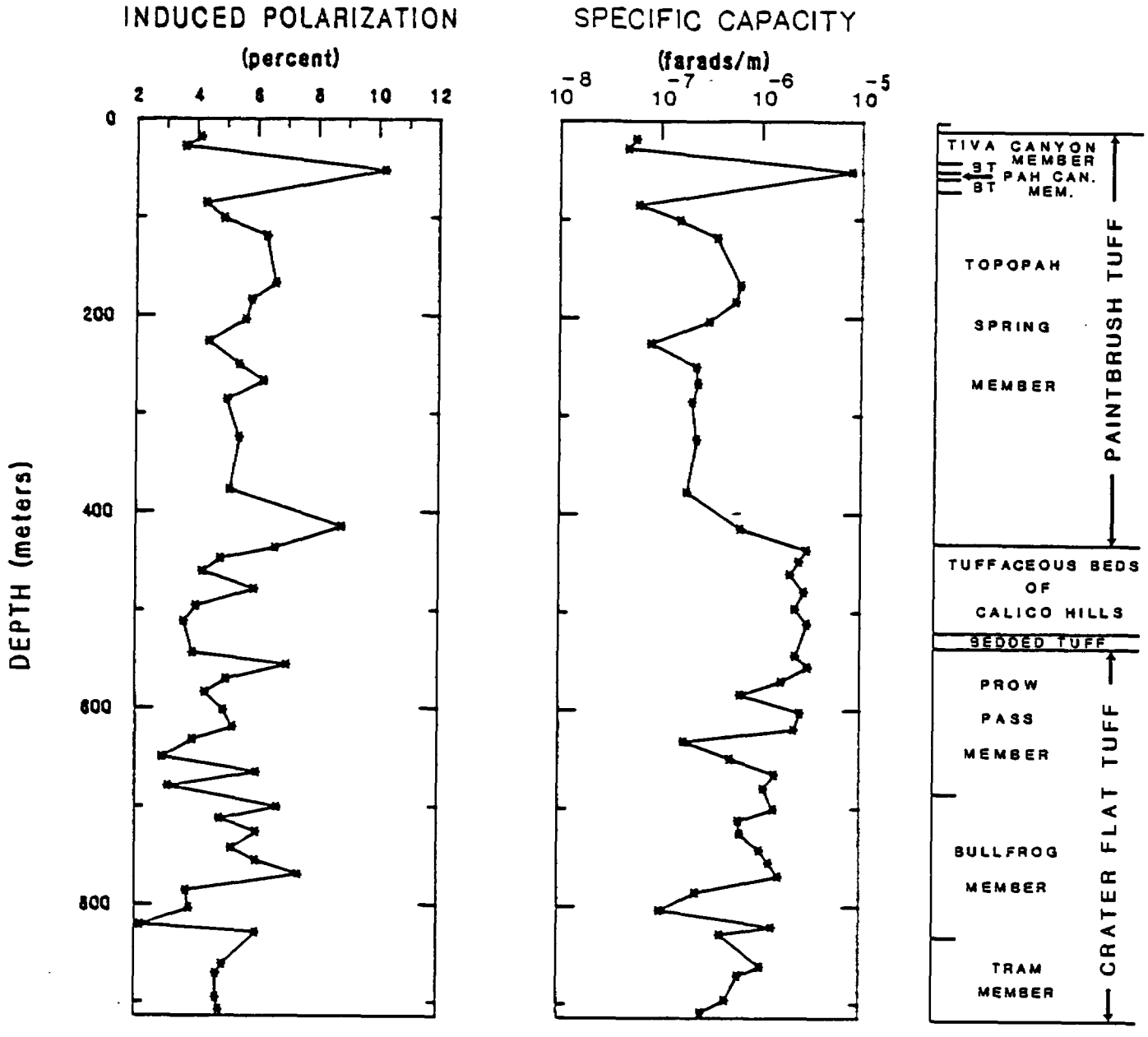

Figure 9. Induced polarization values for USW G-4 core samples plotted against depth of origin. Induced polarization is expressed in terms of percent and as specific capacity in farads/m.

Discussion

Bulk density and resistivity differences between resaturated and natural state sample measurements indicate a somewhat lower saturation level in the natural state samples. This observation holds for samples collected from above and below the water table, which suggests that pore-water loss occurred following core removal from the borehole. Differences in the two comparative measurements are minimal and data sets from either the saturated or natural-state sample collection demonstrate the variability in density and resistivity to be expected in the in place environment.

The patterns of variation indicated on the plots of density, resistivity, and compressional sonic velocity closely follow the plot of porosity, indicating a dependence upon textural rather than compositional changes within the rock. Low porosities are associated with welded and silicified tuffs whereas higher porosities are an indication of non-welded or bedded tuffs. Hence, any one of these properties (density, resistivity, or sonic velocity) is seemingly suitable for characterizing the nature of the rock under investigation.

To test this premise, a least squares line was fitted to the saturated bulk density/porosity relationship for each borehole sample set. The resulting lines of regression for the G-3 and G-4 sample sets, shown in figure 10, define the manner with which the density decreases with increasing porosity. Deviations from the fitted line are caused primarily by pumice content and rock fractures. The data scatter, however, is not pronounced as verified by the correlation coefficient, r, allowing, through use of the calculated linear equation, a reasonably good estimate of rock porosity to be made from density logs. The G-3 and G-4 sample plots are very similar

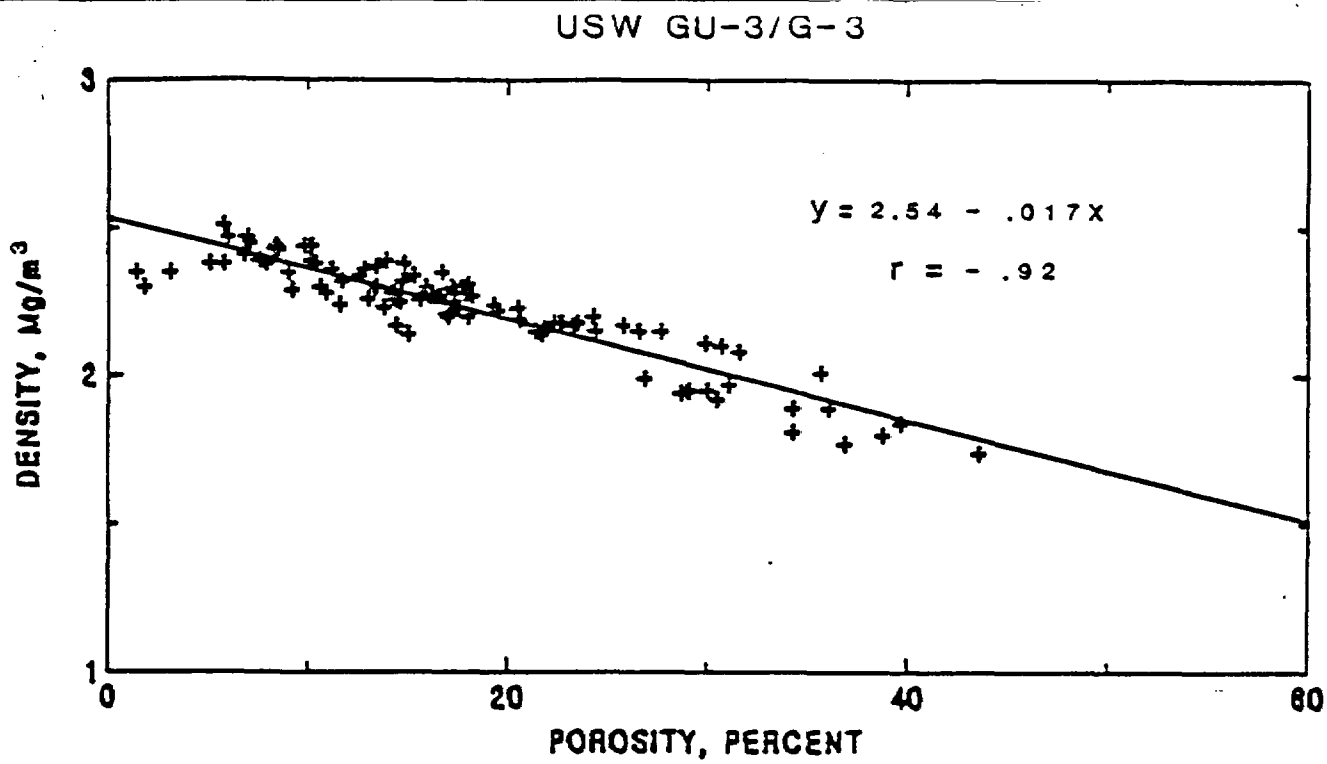

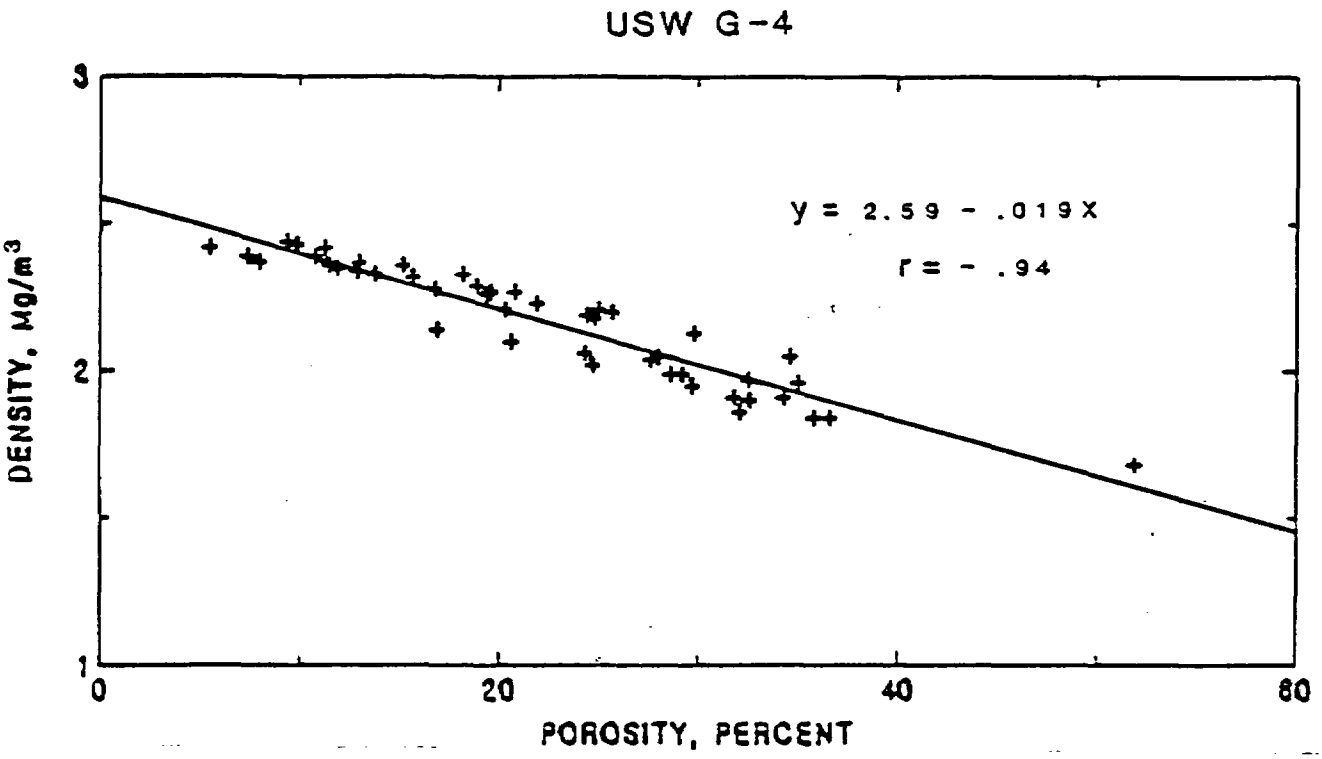

Figure 10. Correlation between density and porosity for the USW GU-3/G-3 and USW G-4 sample data sets based on a least squares fit. The equation for the line of regression and the correlation coefficient, r, is indicated for each plot.

indicating a relative uniformity in the SBD/porosity relationship of the rock over the 2 mile distance separating the boreholes.

A least squares fit between the compressional sonic velocity and porosity data was also made. As with the SBD data, a linear line of regression best defines the correlation between these two rock properties (figure 11). A fairly high degree of scatter is evident on the plot but the correlation coefficient in each case indicates that a trend is clearly established. Fractures, lithophysal cavities, and lithic fragments contained within the rock are the cause of the scatter, hence, the degree to which porosity can reliably be determined from a velocity log is largely dependent upon the homogeneity of the formation.

No linear trend could be established between resistivity and porosity. Resistivity is not only a function of porosity but also of surface conduction owing to the presence of clays and zeolites. The G-4 data can be fitted to a power curve with a high degree of success but the G-3 sample data produced poor results when subjected to the same curve fitting procedure (figure 12). Differences in the regression coefficients determined from both data sets are substantial; therefore, to use either equation to predict porosity values from a resistivity log of a randomly selected Yucca Mountain borehole may prove to be highly inaccurate.

The evaluation of water accessible porosity has been emphasized because of its kinship to hydraulic conductivity which is a critical element in the assessment of a prospective nuclear waste repository. Porosity relating to pore structure is probably not as important to the movement of groundwater within the Paintbrush Tuff, where hydraulic conductivity by means of fracture porosity is predominant. In the Yucca Mountain area the Paintbrush Tuff lies above the static water level so that any waste escaping from materials stored

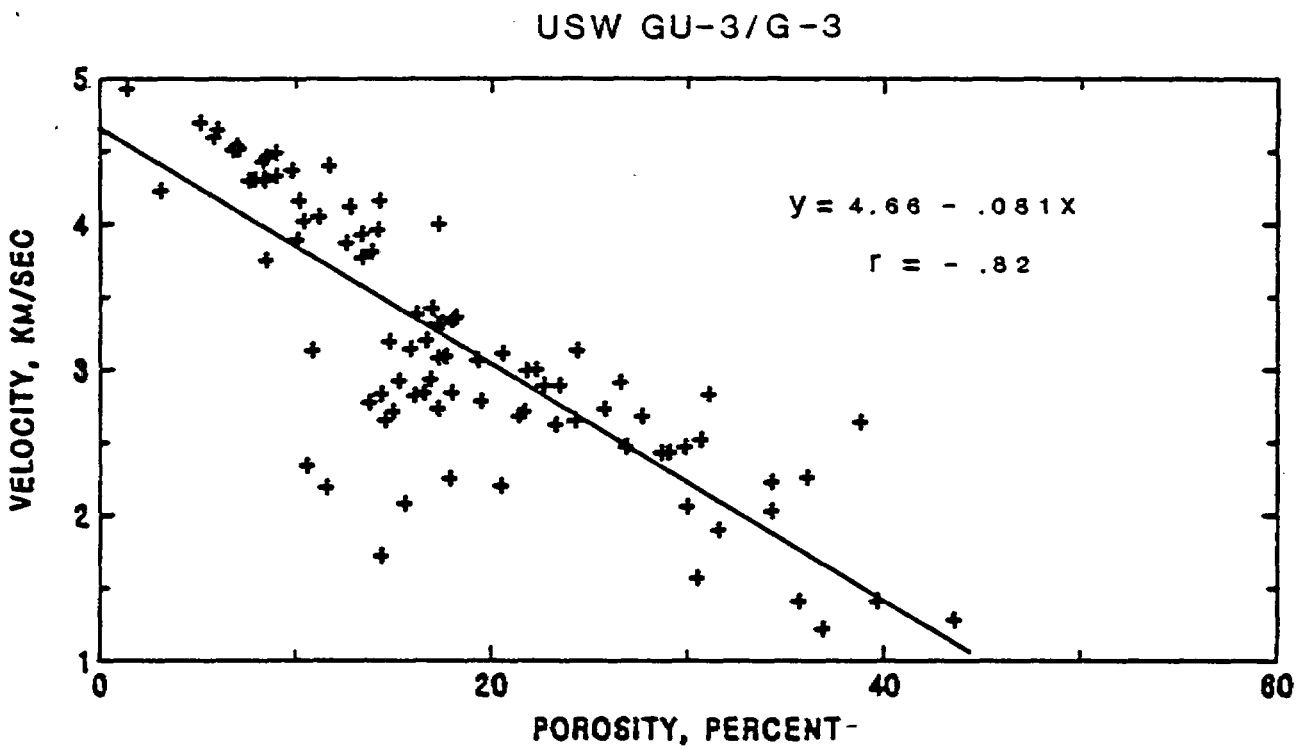

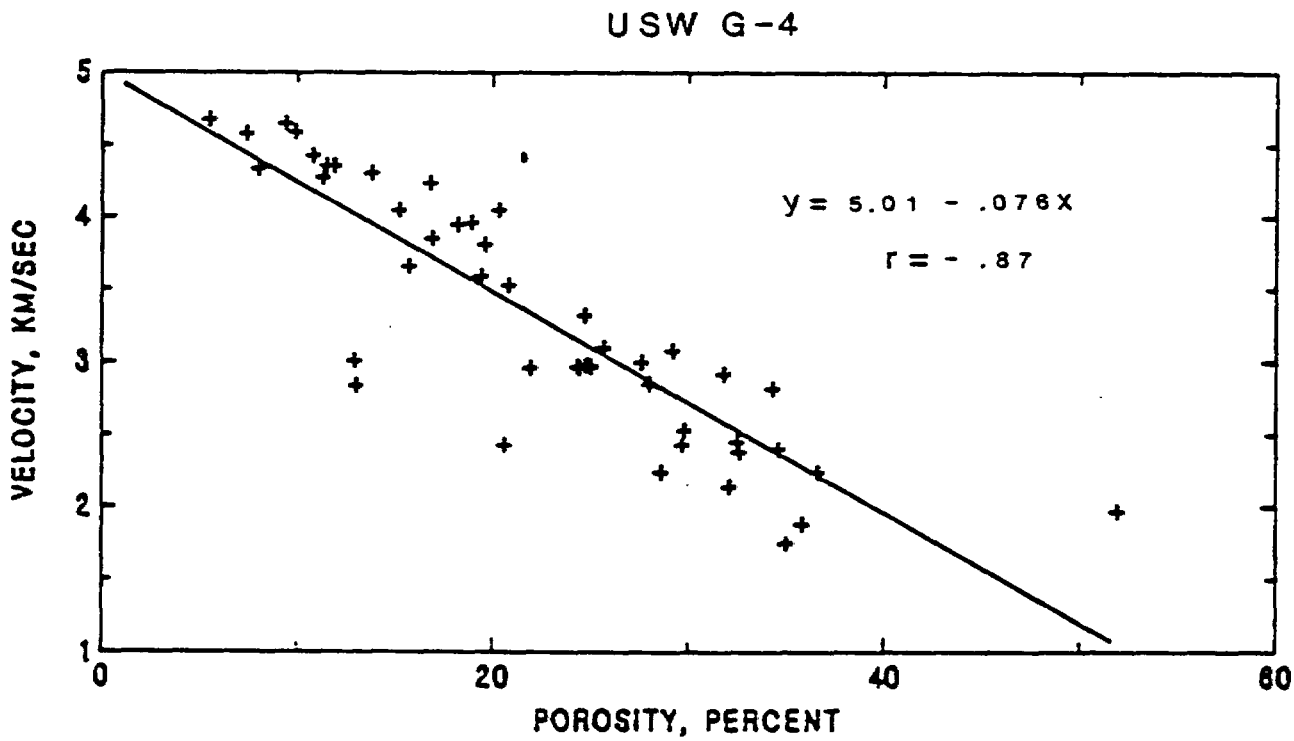

Figure 11. Correlations between velocity and porosity for the USW GU-3/G-3 and USW G-4 sample data sets based on a least squares fit. The equation for the line of regression and the correlation coefficient, r, is indicated for each plot.

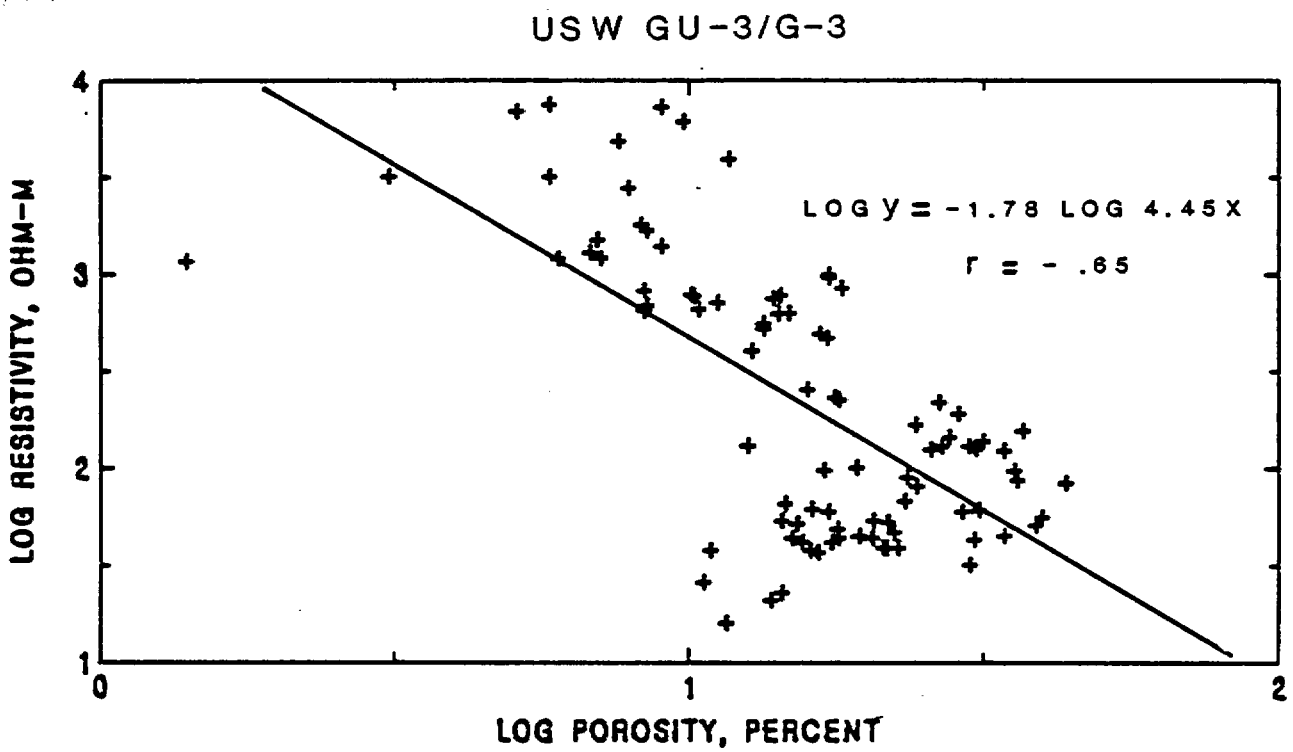

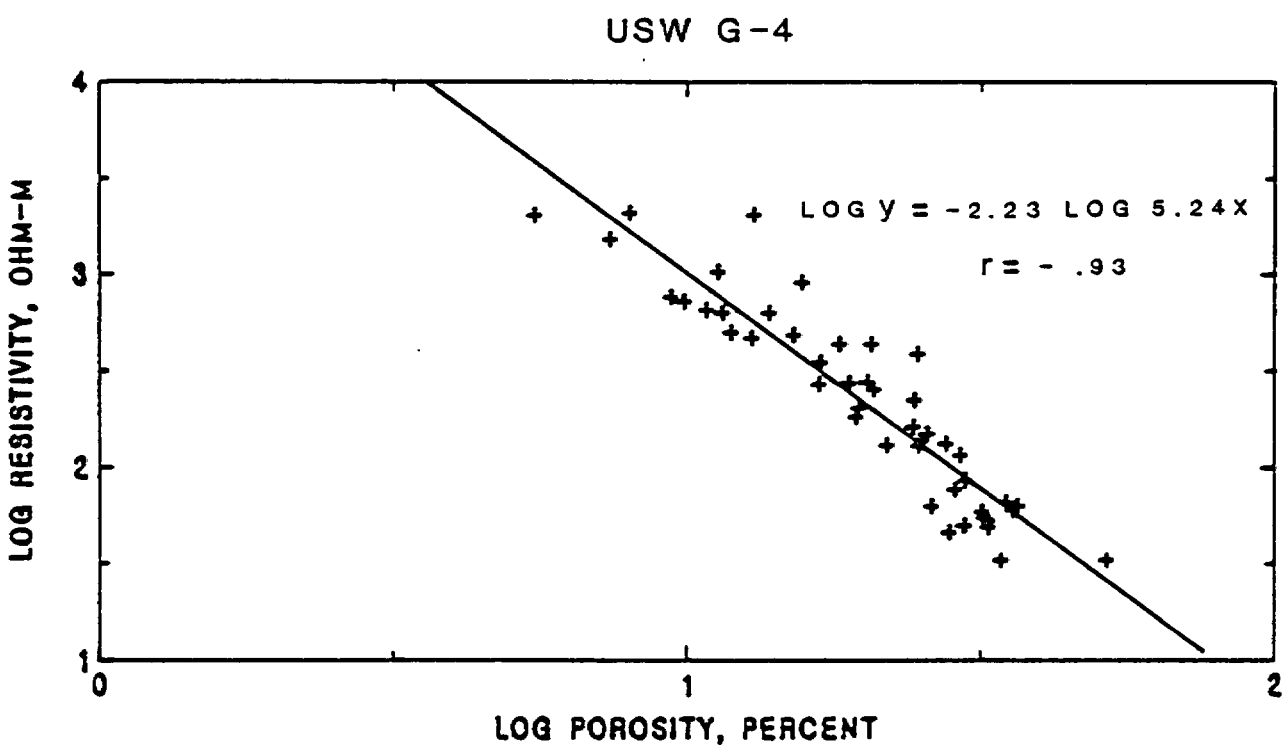

Figure 12. Correlation between resistivity and porosity for the USW G-3/G-3 and USW G-4 sample data sets based on a least squares fit. The equation for the line of regression and the correlation coefficient, r, is indicated for each plot.

in that formation would have to find access to flowing groundwater by means of vertical fractures. The poorly welded tuffs found in the underlying tuffaceous beds of Calico Hills and Crater Flat Tuff have water-accessible porosities in the 20-40 percent range, which provides for relatively easy groundwater movement. However, the abundance of zeolites in these lower formations, as evidenced by the induced polarization response, is sufficient to retard the migration of dissolved radionuclides in the event the waste should come in contact with the groundwater (Wolfsberg and others, 1979).

References

Anderson, L. A., 1981, Rock property analysis of core samples from the Yucca Mountain UE25a-1 borehole, Nevada Test Site, Nevada. U.S. Geological Survey Open-File Report 81-1338.

Carr, W. J., Byers, F. M., and Orkild, Paul P., 1984, Stratigraphic and volcano-tectonic relations of Crater Flat Tuff and some older volcanic units, Nye County, Nevada: U.S. Geological Survey Open-File Report 84-114.

Johnson, G. R., 1979, Textural properties, in Hunt, G. R., Johnson, G. R., Olhoeft, G. R., Watson, D. E., and Watson, K., Initial report of the petrophysics laboratory: U.S. Geological Survey Circular 789, pp 67-74.

Madden, T. R., and Marshall, D. J., 1959, Induced Polarization: A study of its causes and magnitudes in geologic materials. Final Report: RME-3160, Office of Technical Services, Dept. of Commerce, Washington, D.C.

Scott, R. B., and Castellanos, M., 1984, Stratigraphic and structural relations of volcanic rocks in drill hole USW GU-3/G-3, Yucca Mountain, Nye County, Nevada: U.S. Geological Survey Open-File Report. (in review)

Sumner, G. S., 1976, Principles of induced polarization for geophysical exploration. Elsevier Scientific Publishing Co., Amsterdam, Oxford, New York. 277 p.

Wolfsberg, K., Bayhurst, B. P., Crowe, B. M., Daniels, W. K., Erdel, B. R., Lawrence, F. U., Norris, A. E., and Smyth, J. R., 1979, Sorption-desorption studies on tuff: I. Initial studies with samples from the J-13 drill site, Jackass Flats, Nevada, LA-7480-MS. Informal Report, Los Alamos Scientific Laboratory, Los Alamos, New Mexico.